

# Multiple Faults Estimation in Dynamical Systems: Tractable Design and Performance Bounds

Chris van der Ploeg, Mohsen Alirezaei, Nathan van de Wouw, and Peyman Mohajerin Esfahani

**ABSTRACT.** In this article we propose a tractable nonlinear fault isolation filter along with explicit performance bounds for a class of linear dynamical systems in the presence of additive and multiplicative faults. The proposed filter architecture combines tools from model-based approaches in the control literature and regression techniques from machine learning. To this end, we view the regression operator through a system-theoretic perspective to develop operator bounds that are then utilized to derive performance bounds for the proposed diagnosis filter. In the special case of constant faults (both additive and multiplicative), the estimation (tracking) error of the faults signal provably converges to zero with an exponential rate. The performance of the proposed diagnosis filter is validated through an application on the lateral safety systems of SAE level 4 automated vehicles. The numerical results show that the theoretical bounds of this study are indeed close to optimal and potentially tight.

## 1. INTRODUCTION

In dynamical systems, faults are usually considered to cause malicious effects on the input/-output behavior. These effects could potentially result in catastrophic events if not detected and dealt with properly. The diagnosis of faults in dynamical systems is therefore essential to ensure safety of the system. Fault diagnosis methods for faults in dynamical systems can generally be grouped into five different categories [11]. These categories encompass model-based methods, signal-based methods, knowledge-based methods and active fault diagnosis methods which can be applied individually or as a hybrid combination. In this paper we strive to contribute to the state of the art of a hybrid combination of model-based and knowledge-based methods as we touch upon future research topics in the field of active fault diagnosis resulting from insights gained in this research.

The research area of Model-based fault diagnosis has been extensively studied for decades, forming an essential tool to mitigate the need of hardware redundancy, a vision pioneered by Beard in 1971 [3]. In model-based fault diagnosis, a-priori knowledge on the model of the system is assumed, which could be obtained through first-principle modelling or system identification. This model-knowledge can be used to deploy diagnosis algorithms that can, depending on their structure, detect as well as isolate additive-type faults of interest in the form of a *residual*. An example of these algorithms is the bank of estimators, which can be used to detect and isolate faults by making each estimator sensitive to one specific fault or disturbance. This methodology is found in a great variety of

---

*Date:* March 10, 2022.

The authors are with the Department of Mechanical Engineering, Eindhoven University of Technology, ({C.J.v.d.Ploeg, M.Alirezaei, N.v.d.Wouw@tue.nl}@tue.nl), and the Delft Center for Systems and Control, Delft University of Technology (P.MohajerinEsfahani@tudelft.nl).

model-settings, e.g., from single non-linear systems [8] towards multi-agent, possibly large scale, systems [19, 5, 6]. A more integral approach for detection and isolation of faults is an unknown-input type estimator, which decouples the effect of unknown state measurements and disturbances (or faults) from the *residual* through an algebraic approach [16, 9] or approaches using the generalized inverse [1, 27]. Multiplicative faults are inherently more difficult to detect and isolate due to their non-linear appearance in the model, hence, it requires non-linear approaches, e.g., adaptive-type observers [23] or sliding-mode observers [21].

In the field of knowledge-based fault diagnosis, anomalous behavior is detected by comparing the systems behavior with knowledge gained from large sets of historic data [10]. These diagnosis algorithms vary from deep neural network type algorithms [15] up to fundamental supervised-learning algorithms like regression [14]. The latter forms a particularly useful tool for multiplicative fault estimation as its problem setting is identical to the well-known parameter estimation problem in the field of system identification which is often solved using regression [12].

The detection and isolation of additive and multiplicative faults have extensively been studied in the literature as separate phenomena. The combined estimation problem has received little attention in literature and has primarily been focused on the estimation problem of either of the two faults acting non-simultaneous on the same system [26] or the faults acting simultaneously, though, on independent system signals [7]. The case in which both additive and multiplicative faults are simultaneously acting through the same dynamic input/-output relation, while the system is subject to exogenous disturbances, is a particularly difficult case. To the best of our knowledge, this case has not been solved in literature.

**Main Contributions:** The main message of this article revolves around a novel fault diagnosis filter comprising three components of (i) detection, (ii) pre-filter, and (iii) isolation; this architecture will be depicted in Figure 1. The proposed architecture aims to isolate and estimate two additive and multiplicative faults  $f_a$  and  $f_m$  that can potentially be active at the same time. These faults influence the system dynamics in a similar way, and, as such, they are inseparable by means of linear diagnosis tools. In this context, the technical contributions of this study are summarized as follows:

- (i) We develop system-theoretic (error) bounds for the regression operator, a well-known scheme borrowed from the machine learning literature (Proposition 3.3). These bounds play a crucial role to quantify the performance of the proposed diagnosis filter.
- (ii) We propose a general diagnosis architecture as in Figure 1 that comprises three intertwined components. When the component pre-filter is a simple identity operation, we develop an explicit, computable performance bound in terms of the average and variance of the fault signals (Theorem 3.5). In the special case of constants faults, the proposed performance bound sheds light on the inherent tracking errors in terms of the variance of measurement signal (Corollary 3.6).
- (iii) Building on the insight obtained from the performance of the static pre-filter, we propose an alternative design utilizing a dynamic pre-filter and develop the corresponding performance bound (Theorem 3.7). We further show that in the special case of constants faults the estimation error decays to zero exponentially fast (Corollary 3.8).

- (iv) Furthermore, we also develop two technical results concerning the output bounds of linear time-invariant systems with zero steady-state gain (Lemma 3.4) and the variance of product signals (Lemma 4.1) that facilitate the proof of the main results highlighted above. While these results admittedly seem standard, we however did not find them in the literature in the present form as needed for the main results of this study.

Finally, to demonstrate the effectiveness of the proposed methodologies in a real-world application, the theoretical results are validated on a case-study concerning the lateral control for automated vehicles. We show that the proposed performance bounds of the fault diagnosis architecture are rather tight and hence also provide useful insight into when the faults can be provably efficiently estimated in a real-time operation.

The remaining part of this paper is organized as follows. Section 2 introduces the main problem statement and challenges of the research topic; furthermore, an outline of the proposed approach is given. Following the problem statement, the main theoretical results of work are given in Section 3. The theoretical results are backed by technical proofs, which are given in Section 4. In Section 5, the theoretical results are accompanied by numerical simulations, showing the contributions of the set of developed theorems in a more practical daylight. Finally, Section 6 concludes the paper.

**Notation.** The symbols  $\mathbb{N}$  and  $\mathbb{R}$  represent the set of integers and real numbers and the symbol  $\mathbb{R}_+$  represents the set of non-negative real numbers. The  $p$ -norm of a vector  $v$  is denoted by  $\|v\|_p$  where  $p \in [1, \infty]$ . Given a square matrix  $A$  with strictly real eigenvalues, we denote by  $\bar{\lambda} \in \mathbb{R}$  and  $\underline{\lambda} \in \mathbb{R}$  the maximum and minimum eigenvalue values of the matrix, respectively. Given a matrix  $A \in \mathbb{R}^{n \times m}$ , its transpose is denoted by  $A^\top \in \mathbb{R}^{m \times n}$ , the norm  $\|A\|_2 = \bar{\sigma}(A) = \sqrt{\bar{\lambda}(A^\top A)}$  is the largest singular value, and  $A^\dagger := (A^\top A)^{-1} A^\top$  is the pseudo-inverse. Given two matrices with an equal dimension  $A, B \in \mathbb{R}^{m \times n}$ , the operator  $A \circ B \in \mathbb{R}^{m \times n}$  denotes the element-wise (also known as Hadamard) product of two matrices. The operators  $\mu_n[x]$  and  $V_n[x]$  map  $\mathbb{R}$ -valued discrete-time signals to  $\mathbb{R}$ -valued discrete-time signals, and are defined as the first moment  $\mu_n[x](k) := \frac{1}{n} \sum_{i=0}^{n-1} x(k-i)$  and the centered second moment  $V_n^2[x](k) := \frac{1}{n} \sum_{i=0}^{n-1} x^2(k-i) - \mu_n^2[x](k)$  of the signal  $x$  over the last  $n$  time instants. Throughout this study we reserve the bold sub-scripted by  $n$   $\mathbf{x}_n$  as the concatenated version of the signal  $x$  over the last  $n$  time instants:  $\mathbf{x}_n(k) := [x(k), x(k-1), \dots, x(k-n+1)]^\top$ . The symbol  $\mathbf{q}$  represents the shift operator, i.e.,  $\mathbf{q}[x(k)] = x(k+1)$ .

## 2. PROBLEM DESCRIPTION AND OUTLINE OF THE PROPOSED APPROACH

In this section, a formal description of the generic model class along with the basic principles of existing FDI schemes is given. Using this class of models, the high-level problem can be formulated. We further elaborate on the challenges and shortcomings of the current literature. Finally, an outline of the proposed solution is provided, addressing the challenges in the preceding parts.

### 2.1. Model description and problem statement

Throughout this study we consider dynamical systems described via a discrete-time non-linear differential-algebraic equation (DAE) of the form,

$$H(\mathbf{q})[x] + L(\mathbf{q})[z] + F(\mathbf{q})[f_a + E(z)f_m] = 0, \quad (1)$$

where  $x, z, f_a, f_m$  represent discrete-time signals, indexed by the counter  $k$  (e.g.,  $x(k)$ ), taking values in  $\mathbb{R}^{n_x}, \mathbb{R}^{n_z}, \mathbb{R}^{n_f}$ , respectively. The mapping  $E : \mathbb{R}^{n_z} \rightarrow \mathbb{R}^{n_E}$  is a static algebraic mapping capturing the nonlinearity of the dynamics. Let  $n_r$  represent the number of rows in (1), and the matrices  $H(q), L(q), F(q)$  are polynomial functions with  $n_r$  rows and  $n_x, n_z, n_f$  columns in the variable  $q$ , which represents the shift operator. As such, these matrices may be cast as linear operators in the space of discrete-time signals. The signal  $x$  contains all unknown signals in the DAE system, typically comprising the internal states and unknown exogenous disturbances. The signal  $z$  is composed of all known signals including the control inputs  $u$  and the output measurements  $y$ . The signal  $f_a$  represents an additive fault while the signal  $f_m$  is considered to be a multiplicative fault or intrusion which interacts non-linearly with the signal  $E(z)$ . The overall contribution of both fault signals can then be seen in the term  $f_a + E(z)f_m$ , to which we may refer as the “*aggregated fault signal*” hereafter.

The modeling framework (1) encompasses a large class of dynamical systems. A motivating example to show its level of generality is the set of nonlinear ordinary difference equations (ODE) described by

$$\begin{cases} GX(k+1) = AX(k) + B_u u(k) + B_d d(k) + B_f \left( f_a(k) + E_X(B_X X(k), u(k)) f_m(k) \right), \\ y(k) = CX(k) + D_u u(k) + D_d d(k) + D_f \left( f_a(k) + E_Y(B_Y X(k), u(k)) f_m(k) \right), \end{cases} \quad (2)$$

where  $u$  is the input signal,  $d$  the unknown exogenous disturbance,  $X$  the internal state of the system,  $Y$  the measurable output,  $f_a$  the additively acting set of faults or intrusions and finally  $f_m$  the set of faults acting as a multiplication on a non-linear combination of the internal states and input. The matrices  $G, A, B_u, B_d, B_f, B_X, B_Y, C, D_u, D_d$  and  $D_f$  are constant matrices with appropriate dimensions. The following fact provides a simple-to-check condition under which the ODE model (2) falls into the category of our nonlinear DAE model (1).

**Fact 2.1** (From ODE to DAE). *Consider the ODE (2) and suppose there exist matrices  $K_X, K_Y$  such that*

$$\begin{cases} B_X = K_X C, & K_X D_f = 0, & K_X D_d = 0, \\ B_Y = K_Y C, & K_Y D_f = 0, & K_Y D_d = 0. \end{cases} \quad (3)$$

*Then, the ODE model can be viewed as a DAE model (1) by introducing*

$$x = \begin{bmatrix} X \\ d \end{bmatrix}, \quad z = \begin{bmatrix} y \\ u \end{bmatrix}, \quad E(z) = \begin{bmatrix} E_X(K_X(Y - D_u u), u) \\ E_Y(K_Y(Y - D_u u), u) \end{bmatrix},$$

$$H(q) = \begin{bmatrix} -qG + A & B_d \\ C & D_d \end{bmatrix}, \quad L(q) = \begin{bmatrix} 0 & B_u \\ -I & D_u \end{bmatrix}, \quad F(q) = \begin{bmatrix} B_f \\ D_f \end{bmatrix}.$$

Note that from a computational point of view checking the existence condition in (3) is a linear programming (LP) problem, which can be certified highly efficiently.

In the setting described as above, the main objective of this study is as follows.

**Problem statement.** *Consider the DAE system (1) with the available measurement signal  $z$  and the multivariate signal  $f = [f_a, f_m]^T$  comprising both additive and multiplicative faults. We aim to*

design a filter that turns the signal  $z$  to an estimation signal  $\hat{f}$  (i.e., a causal dynamic mapping  $z \mapsto \hat{f}$ ) such that the estimation error  $\|f - \hat{f}\|_2$  is bounded by

$$\|f(k) - \hat{f}(k)\|_2 \leq \mathcal{C}(C_z, C_f, k - k_0),$$

where the constant  $\mathcal{C}$  is an explicit bound depending on the model (1), the parameters  $C_z$  and  $C_f$  representing some characteristics of the measurement  $z$  and fault signals in  $f$ , and the time difference  $k - k_0$  in which  $k_0$  denotes the starting time of the fault signal  $f$  and  $k$  is the current time instant. The signals characteristics can, for instance, include the information of the average and variance of the respective signals.

Throughout this study the following assumption holds, which serves as a necessary and sufficient condition for the detectability of the aggregated fault signal  $f_a + E(z)f_m$  in (1).

**Assumption 2.2** (Detectability). *The polynomial matrices  $H(\mathbf{q})$  and  $F(\mathbf{q})$  in (1) satisfy the rank condition  $\text{Rank}\{[H(\mathbf{q}), F(\mathbf{q})]\} > \text{Rank}\{H(\mathbf{q})\}$ . For simplicity of the exposition, we further assume that  $F(\mathbf{q})$  is a polynomial column vector, i.e.,  $n_{f_a} = n_{f_m} = 1$ .*

Assumption 2.2 paves the way to acknowledge whether the aggregated fault signal is nonzero. However, differentiating the exact contribution between additive fault  $f_a$  and the multiplicative fault introduces nontrivial challenges that we shall discuss in the next section.

## 2.2. State-of-the-art and open challenges

A first step towards the problem of fault isolation is fault detection. To this end, a classical approach is to characterize the *behavioral* set of healthy trajectories. Namely, in absence of the fault signals  $f_a, f_m$ , all possible  $z$ -trajectories of the system can be characterized as

$$\mathcal{M} := \{z : \mathbb{N} \rightarrow \mathbb{R}^{n_z} \mid \exists x : \mathbb{N} \rightarrow \mathbb{R}^{n_x} : H(\mathbf{q})[x] + L(\mathbf{q})[z] = 0\}, \quad (4)$$

which is called the healthy behavior of the system. The goal of the detection process is essentially to determine whether or not the current observed trajectory of  $z$  belongs to  $\mathcal{M}$ . Formally speaking, the detection task is to design a proper system whose input is the known signal  $z$  and the respective output, also referred to as the filter *residual*, is zero when  $z \in \mathcal{M}$  while it is nonzero when the aggregated fault signal  $f_a + E(z)f_m$  is nonzero. In [16], a linear time invariant (LTI) system, also known as a residual generator, is proposed via the use of an irreducible polynomial basis for the nullspace of  $H(\mathbf{q})$ , denoted by  $N_H(\mathbf{q})$ . It is shown that such a polynomial fully characterizes the system behavior (4) in the sense of

$$\mathcal{M} = \{z : \mathbb{N} \rightarrow \mathbb{R}^{n_z} \mid N_H(\mathbf{q})L(\mathbf{q})[z] = 0\}. \quad (5)$$

In order to design a residual generator fulfilling the desired conditions of fault detection it suffices to introduce a linear combination  $N(\mathbf{q}) = \gamma(\mathbf{q})N_H(\mathbf{q})$ , which can be characterized through the following polynomial arguments:

$$N(\mathbf{q})H(\mathbf{q}) = 0, \quad (6a)$$

$$N(\mathbf{q})F(\mathbf{q}) \neq 0. \quad (6b)$$

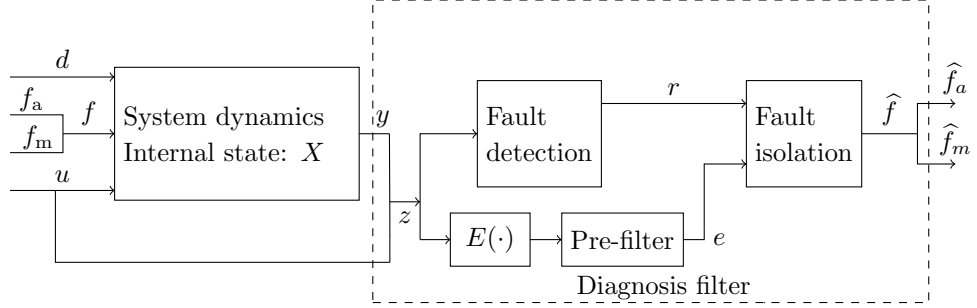


FIGURE 1. Block diagram of the proposed diagnosis.

The first condition (6a) is concerned with the rejection of the natural disturbances and the unknown states, while the second condition (6b) ensures a non-zero of the residual generator response when the fault is non-zero.

In the light of Assumption 2.2, we restrict our attention to a proper LTI diagnosis filter of the form:

$$r := a^{-1}(\mathbf{q})N(\mathbf{q})L(\mathbf{q})[z], \quad (7)$$

where the polynomial row vector  $N(\mathbf{q})$  fulfills the requirements (6), and the stable transfer function  $a^{-1}(\mathbf{q})$  is intended to make the residual generator proper (i.e., the degree of  $a(\mathbf{q})$  is not less than the degree of  $N(\mathbf{q})L(\mathbf{q})$  and stable (i.e., all the zeros of the polynomials  $a(\mathbf{q})$  reside inside in the unit circle). Following the definition of the residual (7) and the DAE model (1), it is not difficult to see that the mapping from the signals  $f_a, f_m$  to the residual  $r$  can be described by

$$r = \mathcal{T}[E(z)f_m + f_a], \quad \text{where} \quad \mathcal{T} := -\frac{N(\mathbf{q})F(\mathbf{q})}{a(\mathbf{q})}. \quad (8)$$

A typical approach to isolate multiple faults ( $f_a, f_m$ ) from one another is to introduce all the faults but one as natural disturbances encoded in the signal  $d$ . However, this technique clearly fails for the DAE systems (1) since Assumption 2.2 does no longer hold. In fact, by virtue of (8), one can see that the residual  $r$  is linearly dependent on both fault signals  $f_a, f_m$ . Due to this linear dependency, the residual can only be sensitive to the aggregated fault signal  $f_a + E(z)f_m$  and it is not possible to isolate this combination by means of linear filters. This is the central fault isolation challenge studied in this work.

### 2.3. Outline of the proposed approach

As mentioned in the preceding section, the key challenge of fault isolation is to decouple the additive fault  $f_a$  and multiplicative fault  $f_m$  when their impact on the dynamics (i.e., the corresponding dynamic matrix  $F(\mathbf{q})$ ) are linearly dependent. In this study, we aim to address this challenge by leveraging tools from the regression theory, a well-known concept from the Machine learning literature [22]. However, in order to integrate those tools in a dynamical system setting and provide rigorous performance guarantees, it is required to view these tools from a system-theoretic perspective and treat them as a dynamical system. This is in fact a main part of the focus in this study.

More specifically, our proposed “*diagnosis filter*” comprises three blocks, see Figure 1. The first block is called “*fault detection*” and its role is to estimate the aggregated signal  $f_a + E(z)f_m$ . This is essentially borrowed from the current literature of fault detection with a slight extension that the residual signal  $r$  is expected to follow the behavior of  $f_a + E(z)f_m$  (rather than only acknowledging the existence of a fault). We call the second block “*fault isolation*” that aims at isolating the contribution of the additive fault signal  $f_a$  and the multiplicative one  $f_m$ . This block is essentially a (nonlinear) regression operator that also receives an additional signal  $e$ , a required regressor signal containing the information of  $E(z)$ . As we will discuss in detail later, the dynamics of the system (and as such the dynamics of  $E(z)$ ) has a nontrivial impact on the performance of the fault isolation block. This effect motivates the inclusion of the third block, to which we refer as the “*pre-filter*”. With regards to the pre-filter, we consider two cases in which one is a trivial identity (i.e.,  $e = E(z)$ ), and the second case is a linear transfer function with the input  $E(z)$ , aiming to compensate for the dynamical behavior between the true aggregated signal and the residual.

### 3. DIAGNOSIS FILTER DESIGN: MAIN RESULTS

As sketched in Figure 1, the proposed diagnosis filter in this study comprises three blocks (i) fault detection, (ii) fault isolation, (iii) pre-filter, which will be elaborated in detail in this section. Here we only discuss the main results and their implications, and we will present the technical preliminaries and proofs in section 4.

#### 3.1. Fault detection: linear residual generators

The following lemma is a slight specialization of [9, Lemma 4.2] that characterizes the class of linear residual generators with a desired asymptotic behavior. In this refined lemma, a steady-state condition on the residual is introduced. This serves as the basis for detection block whose main objective is to detect and track (i.e., estimate) the aggregated fault signal  $f_a + E(z)f_m$ .

**Lemma 3.1** (LP characterization of fault detection). *Consider a polynomial row vector  $N(\mathbf{q}) = \sum_{i=0}^{d_N} N_i \mathbf{q}^i$ , and the system (1) with the model polynomial matrices*

$$H(\mathbf{q}) = \sum_{i=0}^{d_H} H_i \mathbf{q}^i, \quad F(\mathbf{q}) = \sum_{i=0}^{d_F} F_i \mathbf{q}^i, \quad a(\mathbf{q}) = \sum_{i=0}^{d_a} a_i \mathbf{q}^i,$$

where  $d_H, d_F, d_N, d_a$  denote the degree of matrices  $H(\mathbf{q}), F(\mathbf{q}), N(\mathbf{q}), a(\mathbf{q})$ , respectively. Let us define the constant matrices

$$\begin{aligned} \overline{N} &:= \begin{bmatrix} N_0 & N_1 & \dots & N_{d_N} \end{bmatrix}, & \overline{a} &:= \begin{bmatrix} a_0 & a_1 & \dots & a_{d_a} \end{bmatrix} \\ \overline{H} &:= \begin{bmatrix} H_0 & H_1 & \dots & H_{d_H} & 0 & \dots & 0 \\ 0 & H_0 & H_1 & \dots & H_{d_H} & 0 & \vdots \\ \vdots & & \ddots & \ddots & & \ddots & 0 \\ 0 & \dots & 0 & H_0 & H_1 & \dots & H_{d_H} \end{bmatrix}, & \overline{F} &:= \begin{bmatrix} F_0 & F_1 & \dots & F_{d_F} & 0 & \dots & 0 \\ 0 & F_0 & F_1 & \dots & F_{d_F} & 0 & \vdots \\ \vdots & & \ddots & \ddots & & \ddots & 0 \\ 0 & \dots & 0 & F_0 & F_1 & \dots & F_{d_F} \end{bmatrix}. \end{aligned}$$



Under Assumption 2.2, the linear program

$$\begin{cases} \overline{N} \overline{H} = 0, \\ \mathbf{1}^\top \overline{N} \overline{F} = -\mathbf{1}^\top \overline{a}, \end{cases} \quad (9)$$

is feasible and any solution  $\overline{N}$  is an admissible fault detector filter with a zero-steady state error from the aggregated fault to the residual, i.e., for any constant fault signals  $(f_a, f_m)$  and filter initial conditions, the residual (8) fulfills  $\lim_{t \rightarrow \infty} f_a + E(z(t))f_m - r(t) = 0$ .

The proof is omitted as it is a straightforward adaptation from [17, Lemma 4.6].

### 3.2. Fault Isolation: nonlinear regression

Next we present the design of the fault isolation block. A central object of this part is the *regression operator*, a well-known scheme adopted from the machine learning literature [22]. This operator represents the fault isolation block whose domain and range spaces are discrete time signals with appropriate dimensions.

**Definition 3.2** (Regression operator). *Given an integer  $n$  and scalar-valued signals  $e$  and  $r$ , we define*

$$\Phi_n[e, r](k) := \phi_n^\dagger[e](k) \mathbf{r}_n(k), \quad \text{where} \quad \phi_n[e](k) := [\mathbf{e}_n(k), \mathbf{1}_n] \in \mathbb{R}^{n \times 2}, \quad (10)$$

with the ones vector  $\mathbf{1}_n := [1, 1, \dots, 1]^\top \in \mathbb{R}^n$  and the operator  $^\dagger$  as the pseudo-inverse.<sup>1</sup>

In the context of the fault diagnosis scheme in Figure 1, the output  $\Phi_n[e, r](k)$  of the nonlinear regression operation in Definition 3.2 is, in fact, equal to the fault estimate  $\hat{f}$ . The nonlinear regression operator in Definition 3.2 enjoys certain regularity properties that are key for the results we will develop later. The following proposition provides input-output bounds of the regression operator. These bounds will be utilized later to develop a performance bound for the proposed diagnosis filter in a real-time and dynamic operational mode.

**Proposition 3.3** (Regression bounds). *Consider the regressor operator in Definition 3.2. For all discrete-time scalar-valued signals  $r, e$  and  $y = [y^{(1)}, y^{(2)}]^\top$ , at each time instant  $k \in \mathbb{N}$  where  $V_n[e] \neq 0$  it holds that*

$$\|\Phi_n[e, y^{(1)} + e y^{(2)}] - \mu_n[y]\|_2 \leq \frac{\mathcal{C}_n(\mathbf{e}_n)}{V_n[e]} \left( V_n[y^{(1)}] + V_n[y^{(2)}] \|\mathbf{e}_n\|_\infty \right), \quad (11a)$$

$$\|\Phi_n[e, r]\|_2 \leq \frac{\mathcal{C}_n(\mathbf{e}_n)}{\sqrt{n} V_n[e]} \|\mathbf{r}_n\|_2, \quad (11b)$$

where the constant is defined as  $\mathcal{C}_n(\mathbf{e}_n) := \sqrt{V_n^2[e] + \mu_n^2[e] + 1}$ .

*Proof.* The proof is provided in Section 4.1. □

We emphasize that the bounds in (11) hold for each time instant  $k \in \mathbb{N}$ , but to avoid clutter we drop the time-dependency of the signals (e.g.,  $\Phi_n[e, r]$  instead of  $\Phi_n[e, r](k)$ ). We also note that the parameter  $\mathcal{C}$  only depends on the signal  $e$  (more precisely, on the last  $n$  time instants of the signal  $e$

<sup>1</sup> $A^\dagger := (A^\top A)^{-1} A^\top$ .



denoted by  $\mathbf{e}_n$ ). In this view, the inequality (11b) indeed represents an operator norm for the linear mapping  $r \mapsto \Phi_n[e, r]$ . Let us elaborate further how the bounds as in (11) are the first stepping-stones towards our main goal in this study. Measuring the “aggregated” signal  $y^{(1)} + e y^{(2)}$ , one can utilize the bound in (11a) to bound the error on the estimation of the average of the multivariate signal  $y = [y^{(1)}, y^{(2)}]^\top$  (i.e.,  $\mu_n[y]$ ) via the regression operator. It is worthwhile to note that when the signal  $y$  is constant, then  $y = \mu_n[y]$  and  $V_n[y^{(1)}] = V_n[y^{(2)}] = 0$ , and that the estimation error reduces to zero provided that  $V_n[e] \neq 0$ . The second result (11b) allows us to bound the output of the nonlinear regression operator given a bounded input, which can be viewed as a means to bound estimated faults given the dynamically filtered residual  $r$  as an input. The bounds (11) in fact offer a rigorous framework to treat the isolation block as a nonlinear dynamical system whose induced gain, and as such the boundedness of its output, is determined by  $V_n[e]$ , the variance of signal  $e$  over a horizon with the length  $n$ .

### 3.3. Pre-filter: dynamic compensator

In this section, we focus on the pre-filter block in Figure 1. Before presenting the main results of this paper, we first need to proceed with a basic preparatory lemma on the output bound of LTI systems. To improve the flow of the paper, we skip the technical proofs of the results in this section and defer them to Section 4.3.

**Lemma 3.4** (Zero steady-state LTI output bound). *Consider a proper LTI system with the numerator  $b(\mathbf{q}) = \sum_{i=0}^d b_i \mathbf{q}^i$ , and the denominator  $a(\mathbf{q}) = \prod_{i=1}^d (\mathbf{q} - p_i)$  where the poles are distinct and the dominant one (i.e., the one closest to the unit circle) is  $|p| < 1$ . Suppose the steady-state gain of the filter is 0 (i.e.,  $b(1) = 0$ ), the internal state (in the Jordan canonical form) is initiated at  $X(0)$ , and the input signal  $u(t)$  is 0 until time  $k_0$  and takes possibly nonzero values for  $t \geq k_0$ . Then, the output signal  $y(t)$  satisfies the bound*

$$\|y_n\|_2 \leq C_0 \|X(0)\|_2 |p|^{k-n} + C_1 \|\mu_{k-k_0}[u]\|_2 |p|^{k-n-k_0} + C_2 \sqrt{k-k_0} V_{k-k_0}[u],$$

where the constants  $C_0, C_1, C_2$  are defined as

$$r_i = \frac{b(-p_i)}{\prod_{j \neq i} (p_j - p_i)}, \quad C_0 = \sqrt{n \sum_{i=1}^d r_i^2}, \quad C_1 = \frac{\sqrt{n d \sum_{i=1}^d r_i^2}}{1 - |p|}, \quad C_2 = |b_d| + \sum_{i=1}^d \frac{|r_i|}{1 - |p_i|}.$$

*Proof.* The proof is provided in Section 4.1. □

The statement of Lemma 3.4 is rather classical and is not really unexpected. However, we need such an assertion with explicit computable bounds for the main results of this study, which to our best knowledge does not exist in this form in the literature.

We further propose two possible designs for the pre-filter, each of which comes along with certain pros and cons. The first, and simplest, design option is the static identity block. The next theorem presents a performance bound for this static pre-filter design.

**Theorem 3.5** (Performance bound: (I) static pre-filter). *Consider the system (1) and the fault diagnosis filter in Figure 1 where the fault detection block is characterized by the linear program (9) and a denominator  $a(\mathbf{q})$  with distinct and real-valued poles. The fault isolation block is the regression*

operator in (10) with the horizon  $n$ . Suppose the pre-filter block is identity (i.e.,  $e = E(z)$ ), and the fault signal starts at time  $k_0$ . Then, at each time instant  $k \in \mathbb{N}$  we have

$$\|\hat{f} - \mu_n[f]\|_2 \leq \frac{1}{V_n[e]} \left( \alpha_0 |p|^{k-k_0} + \alpha_1 V_{k-k_0}[f_a] + \alpha_2 V_{k-k_0}[f_m] + \alpha_3 \right), \quad (12a)$$

where the constant  $p \in \mathbb{R}$  is the dominant pole of the denominator  $a(q)$  and the involved constants are defined as

$$\alpha_0 = \mathcal{C}_1 \frac{\mathcal{C}_n(\mathbf{e}_n)}{\sqrt{n}} \left( |\mu_{k-k_0}[f_a]| + |\mu_{k-k_0}[ef_m]| \right), \quad (12b)$$

$$\alpha_1 = \mathcal{C}_2 \mathcal{C}_n(\mathbf{e}_n) \sqrt{\frac{k-k_0}{n}}, \quad (12c)$$

$$\alpha_2 = \mathcal{C}_2 \mathcal{C}_n(\mathbf{e}_n) \sqrt{\frac{k-k_0}{n}} \left( \sqrt{k-k_0} V_{k-k_0}[e] + |\mu_{k-k_0}[e]| \right), \quad (12d)$$

$$\alpha_3 = \mathcal{C}_n(\mathbf{e}_n) \left( V_n[f_a] + V_n[f_m] \|\mathbf{e}_n\|_\infty + \mathcal{C}_2 \sqrt{\frac{k-k_0}{n}} |\mu_{k-k_0}[f_m]| V_{k-k_0}[e] \right). \quad (12e)$$

in which  $\mathcal{C}_n(\mathbf{e}_n)$  is defined in Proposition 3.3 and the constants  $\mathcal{C}_1, \mathcal{C}_2$  are defined in Lemma 3.4.

*Proof.* The proof is provided in Section 4.3, which builds on an additional preliminary lemma in Section 4.2.  $\square$

By virtue of Theorem 3.5, one can inspect how different aspects of the proposed design contribute to the fault estimation error. The most critical term is  $V_n[e]$  in the denominator of the right-hand side of (12a). This challenging dependency is, however, an inherent limitation of the desired isolation task. In fact, one can show that when the signal  $E(z)$  is constant (i.e.,  $V_n[e] \equiv 0$ ), separation of the two faults  $(f_a, f_m)$  is even theoretically impossible. To reinforce this statement, consider the case  $V_n[e] \equiv 0$  with arbitrary faults  $f_a$  and  $f_m$ . It can be observed that the regression operator (10) contains the inverse of a degenerate component  $\phi_n[e]^\top \phi_n[e]$  which, by definition, does not exist in such a case. This result shows that the signal  $e$ , over horizon  $n$ , does then not span the behavior of the aggregated fault over the same horizon, a concept close to the well-known *persistence of excitation* phenomena for LTI systems [24]. The term  $\alpha_0$  in (12b) reflects the contribution of the average behavior of fault signals. In (12b) it can be seen that this term diminishes exponentially fast after the start of the fault signal due to its proportionality with the exponentially decaying term containing the dominant pole  $|p|$  of the stable denominator  $a(q)$ . In this light, we can deduce that the impact of these average behaviors on the performance is in fact negligible. The terms concerning  $\alpha_1$  and  $\alpha_2$  in (12) are mainly influenced by the variance of the fault since the beginning of the fault. The contribution of these variances in combination with the dynamics constants  $\mathcal{C}_1, \mathcal{C}_2$  from Lemma 3.4 is also an inevitable factor in the estimation error, since the regression model in Definition 3.2 assumes constant contributions of the faults  $f_a$  and  $f_m$  appearing through the transfer function (8) in the residual  $r$  over a horizon  $n$ . Finally, the last term involving  $\alpha_3$  is a critical and potentially persistent source of error. In particular, the variance signal  $V_{k-k_0}[e]$  introduces a non-zero estimation error even in the case of constant fault signals. The next corollary highlights this effect.

**Corollary 3.6** (Constant faults: part I). *Consider the system and the diagnosis filter as in Theorem 3.5. Suppose the fault signals are constant  $f = (\bar{f}_a, \bar{f}_m)$ , starting from the time  $k_0$ . Then, for any time instant  $k \geq k_0 + n$  we have*

$$\|\hat{f} - f\|_2 \leq \frac{\mathcal{C}_n(\mathbf{e}_n)}{\sqrt{n}V_n[e]} \left( \mathcal{C}_1(|\bar{f}_a| + |\bar{f}_m|\mu_{k-k_0}[e])|p|^{k-n-k_0} + \mathcal{C}_2\sqrt{k-k_0}|\bar{f}_m|V_{k-k_0}[e] \right). \quad (13)$$

*Proof.* The proof is a direct application of Theorem 3.5. Under the assumption that the fault signals are constants after time  $k \geq k_0$ , we know that  $V_{k-k_0}[f_a] = V_{k-k_0}[f_m] = 0$ . Moreover, assuming further that  $k \geq n + k_0$ , we can also conclude that  $V_n[f_a](k) = V_n[f_m](k) = 0$ . In addition, the average terms of the signal reduces to  $\mu_{k-k_0}[f_a] = \bar{f}_a$  and  $\mu_{k-k_0}[f_m] = \bar{f}_m$ . Substituting these quantities in the bound (12) concludes (13).  $\square$

As noted above, the variance of the signal  $e$  is a persistent factor contributing to the performance bound, which is captured by the last term on the right-hand side of the inequality (13). This is somehow expected due to the causality effect of the system dynamics. More specifically, the residual  $r$ , the output of the fault detection block, opts to follow the aggregated fault signal  $f_a + E(z)f_m$  but it relies on the dynamics  $\mathcal{T}(\mathbf{q})$  (cf., (8)). However, when the pre-filter is set to identity (i.e.,  $e = E(z)$ ), the information of the signal is provided instantly for the isolation block (due to the static identity pre-filter), rendering some persistent potential error proportional to  $V_{k-k_0}[e]$ . This error exists due to the fact that the fault isolation block assumes a static mapping  $e \mapsto r$  for the static pre-filter case, whereas this mapping is inherently dynamic due to the dynamics of the system and the fault detection block (8). This dynamical misalignment in the fault isolation block manifests itself in the estimation error, even for constant faults, as shown in (13). Next, we aim to address this issue by filtering the information of the signal  $E(z)$  through the same dynamics that the residual of detection filter experiences. This novel viewpoint brings us to the second choice of pre-filter next.

**Theorem 3.7** (Performance bound: (II) dynamic pre-filter). *Consider the system (1) and the fault diagnosis filter in Figure 1 where the fault detection block is characterized by the linear program (9) and a denominator  $a(\mathbf{q})$  with distinct and real-valued poles. The fault isolation block is the regression operator in (10) with the horizon  $n$ . Suppose the pre-filter block is the linear system  $\mathcal{T}$  as defined in (8) (i.e.,  $e = \mathcal{T}[E(z)]$ ) with the internal states denoted by  $X_p$ . If the fault signal starts at time  $k_0$ , then at each time instant  $k \in \mathbb{N}$  we have*

$$\|\hat{f} - \mu_n[f]\|_2 \leq \frac{1}{V_n[e]} \left( \beta_0|p|^{k-k_0} + \beta_1V_{k-k_0}[f_a] + \beta_2V_{k-k_0}[f_m] + \beta_3 \right), \quad (14a)$$

where the constant  $p \in \mathbb{R}$  is the dominant pole of the denominator  $a(\mathbf{q})$  and the involved constants are defined as

$$\beta_0 = \frac{\mathcal{C}_n(\mathbf{e}_n)}{\sqrt{n}} \left( \mathcal{C}_1(|\mu_n[f_a]| + |\mu_{k-k_0}[E(z)f_m] - \mu_{k-k_0}[E(z)]\mu_n[f_m]|) + \mathcal{C}_0|\mu_n[f_m]| \|X_p(k-k_0)\|_2 \right), \quad (14b)$$

$$\beta_1 = \mathcal{C}_2\mathcal{C}_n(\mathbf{e}_n)\sqrt{\frac{k-k_0}{n}}, \quad (14c)$$

$$\beta_2 = \mathcal{C}_2\mathcal{C}_n(\mathbf{e}_n)\sqrt{\frac{k-k_0}{n}} \left( \sqrt{k-k_0}V_{k-k_0}[e] + |\mu_{k-k_0}[e]| \right), \quad (14d)$$

$$\begin{aligned} \beta_3 = \mathcal{C}_n(\mathbf{e}_n) & \left( V_n[f_a] + V_n[f_m] (\|\mathbf{e}_n\|_\infty + \|\mathbf{e}_n - E(\mathbf{z}_n)\|_\infty) \right. \\ & \left. + \mathcal{C}_2 \sqrt{\frac{k-k_0}{n}} |\mu_{k-k_0}[f_m] - \mu_n[f_m]| V_{k-k_0}[E(z)] \right). \end{aligned} \quad (14e)$$

in which  $\mathcal{C}_n(\mathbf{e}_n)$  is defined in Proposition 3.3, the constants  $\mathcal{C}_0, \mathcal{C}_1, \mathcal{C}_2$  are defined in Lemma 3.4, and the vector-valued signal  $E(\mathbf{z}_n)$  is understood as the evaluation of the function  $E(\cdot)$  on each of the elements of the vector  $\mathbf{z}_n$ .

*Proof.* The proof is provided in Section 4.3, which builds on an additional preliminary lemma in Section 4.2.  $\square$

In a comparison with Theorem 3.5, one can see that the main difference in the fault estimation error bound appears in the last coefficient of the error bounds (cf,  $\alpha_3$  in (12a) and  $\beta_3$  in (14a)). In particular, the idea of an appropriate dynamic pre-filter allows us to shift the contribution of the variance signal  $V_{k-k_0}[e]$  to the third term related to  $\beta_2$  in (14d), which is multiplied by the variance of the multiplicative fault  $V_{k-k_0}[f_m]$ . This shift has a significant impact on the performance when the fault signals are constant during the activation time (i.e.,  $k \geq k_0$ ). Before proceeding with the simplification of the result in this case, let us note that the dynamic pre-filter does not necessarily outperform the static one proposed by Theorem 3.5 due to the difference in the term  $V_n[e]$ . Indeed, the filtered signal  $\mathcal{T}[E(z)]$  may have a lower variance, which has a negative impact on the performance bounds.

**Corollary 3.8** (Constant faults: part II). *Consider the system and the diagnosis filter as in Theorem 3.7. Suppose the fault signals are constant  $(\bar{f}_a, \bar{f}_m)$  starting at time  $k_0$ . Then, for any time instant  $k \geq k_0 + n$*

$$\|\hat{f} - f\|_2 \leq \frac{\mathcal{C}_n(\mathbf{e}_n)}{\sqrt{n}V_n[e]} \left( \mathcal{C}_1|\bar{f}_a| + \mathcal{C}_0|\bar{f}_m| \|X_p(k_0)\|_2 \right) |p|^{k-k_0}. \quad (15)$$

*Proof.* In parallel to Corollary 3.6, the proof is a direct application of Theorem 14 when the fault signals are constants after time  $k \geq n + k_0$ , and as such  $V_{k-k_0}[f_a] = V_{k-k_0}[f_m] = 0$ ,  $V_n[f_a](k) = V_n[f_m](k) = 0$ ,  $\mu_{k-k_0}[f_a] = \bar{f}_a$  and  $\mu_{k-k_0}[f_m] = \bar{f}_m$ . Besides, we also note that the term  $\mu_{k-k_0}[f_m] - \mu_n[f_m] = 0$  vanishes as well. Substituting these quantities in the bound (14) concludes (15).  $\square$

In the case of constant faults, Corollary 3.8 indicates that the fault estimation error goes to zero exponentially fast if the filtered signal  $e$  behaves “nicely” (i.e.,  $V_n[e]$  is uniformly away from zero). In comparison with the assertion of Corollary 3.6, this outcome evidently highlights the role of the dynamic pre-filter on the diagnosis performance.

Let us close this section by a brief summary of the results. In this section, a general diagnosis architecture has been proposed. System theoretic bounds for the regression operator (Definition 3.2) and the LTI bound (Lemma 3.4) have been used for the construction of guaranteed performance bounds for two pre-filter variants within this diagnosis architecture. The insights gained from the first pre-filter variant (i.e., the identity block in Theorem 3.5) and its behavior for constant faults (Corollary 3.6), have been leveraged to propose a second design variant (i.e., the dynamic pre-filter in Theorem 3.7), which has been proven to have an exponentially decaying performance bound for constant faults (Corollary 3.8).

#### 4. TECHNICAL PRELIMINARIES AND PROOFS OF MAIN RESULTS

This section presents the technical proofs of the theoretical results in Section 3. To this end, we will also provide some preliminary results to facilitate the proof of the main results.

##### 4.1. Proofs of the regression and LTI output bounds

*Proof of Proposition 3.3.* From (10) recall that the matrix  $\phi_n^\dagger[e]$  is the pseudo-inverse of  $\phi_n[e]$ , and using the spectral norm properties we have

$$\begin{aligned}\|\phi_n^\dagger[e]\|_2 &= \bar{\sigma}(\phi_n^\dagger[e]) = \sqrt{\bar{\lambda}(\phi_n^{\dagger\top}[e]\phi_n^\dagger[e])} = \sqrt{\bar{\lambda}((\phi_n^\top[e]\phi_n[e])^{-1}\phi_n^\top[e]\phi_n[e](\phi_n^\top[e]\phi_n[e])^{-1})}, \\ &= \sqrt{\bar{\lambda}((\phi_n^\top[e]\phi_n[e])^{-1})} = \sqrt{(\underline{\lambda}(\phi_n^\top[e]\phi_n[e]))^{-1}},\end{aligned}\quad (16)$$

where  $\bar{\lambda}$  and  $\underline{\lambda}$  represent the maximum and minimum eigenvalues, respectively. Based on Definition 3.2, the matrix  $\phi_n^\top[e]\phi_n[e] \in \mathbb{R}^{2 \times 2}$  can be expanded as

$$\phi_n^\top[e]\phi_n[e] = \begin{bmatrix} \sum_{i=0}^{n-1} (e(k-i))^2 & \sum_{i=0}^{n-1} e(k-i) \\ \sum_{i=0}^{n-1} e(k-i) & n \end{bmatrix} = n \begin{bmatrix} V_n^2[e] + \mu_n^2[e] & \mu_n[e] \\ \mu_n[e] & 1 \end{bmatrix}.$$

Following some straightforward algebraic computations, one can find the minimum eigenvalue of the above matrix, yielding the bound of (16) as

$$\|\phi_n^\dagger[e]\|_2 = \sqrt{\frac{2}{n(a - \sqrt{a^2 - b})}} = \sqrt{\frac{2(a + \sqrt{a^2 - b})}{nb}}, \quad a := 1 + V_n^2[e] + \mu_n^2[e], \quad b := 4V_n^2[e].$$

Using the trivial bound  $\sqrt{a^2 - b} \leq |a|$ , we arrive at the upper bound

$$\|\phi_n^\dagger[e]\|_2 \leq \frac{\sqrt{1 + V_n^2[e] + \mu_n^2[e]}}{\sqrt{n} V_n[e]} = \frac{\mathcal{C}_n(\mathbf{e}_n)}{\sqrt{n} V_n[e]}. \quad (17)$$

Given the upper bound above and following Definition 3.2, we can rewrite the regression operator as

$$\begin{aligned}\Phi_n[e, y^{(1)} + e y^{(2)}] &= \phi_n^\dagger[e] (\mathbf{y}_n^{(1)} + \mathbf{e}_n \circ \mathbf{y}_n^{(2)}) \\ &= \phi_n^\dagger[e] (\mu_n[y^{(1)}] \mathbf{1}_n + \mu_n[y^{(2)}] \mathbf{e}_n - \mu_n[y^{(1)}] \mathbf{1}_n + \mu_n[y^{(2)}] \mathbf{e}_n - \mu_n[y^{(2)}] \mathbf{e}_n). \quad (18)\end{aligned}$$

where the operator  $\circ$  is the element-wise product between the vectors with an equal dimension. We note that when  $V_n[e] > 0$ , the matrix  $\phi_n[e]$  is full rank, and that its pseudo-inverse  $\phi_n^\dagger[e]$  is a well-defined object. Moreover, by virtue of the basic definition of the regression operator in (10), it is not difficult to observe that

$$\phi_n^\dagger[e] (\mu_n[y^{(1)}] \mathbf{1}_n + \mu_n[y^{(2)}] \mathbf{e}_n) = [\mu_n[y^{(1)}], \mu_n[y^{(2)}]]^\top = \mu_n[y^{(1)}, y^{(2)}]^\top = \mu_n[y]. \quad (19)$$

The interpretation of (19) is that if the coefficients of the signal  $e$  is constant over a horizon with length  $n$  (i.e.,  $\mu_n[y^{(1)}], \mu_n[y^{(2)}]$ ), then the regression operator at each time instant retrieves these constants providing that the signal  $e$  has nonzero variance over the same horizon (i.e.,  $V_n[e] > 0$ ). The observation (19) allows us to simplify the relation (18) to

$$\Phi_n[e, y^{(1)} + e y^{(2)}] = \phi_n^\dagger[e] (\mathbf{y}_n^{(1)} - \mu_n[y^{(1)}] \mathbf{1}_n + \mathbf{e}_n \circ (\mathbf{y}_n^{(2)} - \mu_n[y^{(2)}] \mathbf{1}_n)) + \mu_n[y].$$

Bringing the term  $\mu_n[y](k)$  to the left-hand side and using the triangle inequality leads to

$$\begin{aligned}\|\Phi_n[e, y^{(1)} + e y^{(2)}] - \mu_n[y]\|_2 &\leq \|\phi_n^\dagger[e]\|_2 \left\| \mathbf{y}_n^{(1)} - \mu_n[y^{(1)}] \mathbf{1}_n + \mathbf{e}_n \circ \left( \mathbf{y}_n^{(2)} - \mu_n[y^{(2)}] \mathbf{1}_n \right) \right\|_2 \\ &\leq \|\phi_n^\dagger[e]\|_2 \left( \left\| \mathbf{y}_n^{(1)} - \mu_n[y^{(1)}] \mathbf{1}_n \right\|_2 + \left\| \mathbf{e}_n \circ \left( \mathbf{y}_n^{(2)} - \mu_n[y^{(2)}] \mathbf{1}_n \right) \right\|_2 \right) \\ &= \|\phi_n^\dagger[e]\|_2 \left( \sqrt{n} \left( V_n[y^{(1)}] + V_n[y^{(2)}] \|\mathbf{e}_n\|_\infty \right) \right).\end{aligned}$$

Substituting the upper bound (17) in the above inequality concludes the first assertion (11a). The second claim (11b) is a direct consequence of the upper bound (17) as follows:

$$\|\Phi_n[e, r]\|_2 = \|\phi_n^\dagger[e] \mathbf{r}_n\|_2 \leq \|\phi_n^\dagger[e]\|_2 \|\mathbf{r}_n\|_2 \leq \frac{\mathcal{C}_n(\mathbf{e}_n)}{\sqrt{n} V_n[e]} \|\mathbf{r}_n\|_2.$$

This concludes the proof of Proposition 3.3.  $\square$

The second part of this section is concerned with the lemma about the LTI output bounds with zero steady-state.

*Proof of Lemma 3.4.* Given a time instant  $k \in \mathbb{N}$ , we decompose the time-varying control signal to two parts

$$u(k) = (u(k) - \bar{u} \delta_{k_0}(k)) + \bar{u} \delta_{k_0}(k), \quad (20)$$

where the constant is set to  $\bar{u} = \mu_{k-k_0}[u](k)$  and  $\delta_{k_0}(k) = 1$  if  $k \geq k_0$ ; otherwise  $= 0$ . That is, the second input  $\bar{u} \delta_{k_0}$  is seen as a constant input in the interval  $t \in [k_0, k]$ . Leveraging the superposition property of the linear systems, one can view the outcome signal of the system as the response to the two different inputs in (20). In the first step, we focus on the response of the constant input signal  $\bar{u} \delta_{k_0}$  that starts from  $k_0$ .

Let  $(A, B, C, D)$  be a state-space realization of the LTI system. Note that by 0-steady state property, we know that  $D = -C(I - A)^{-1}B$ . Utilizing the state-space description directly, we can rewrite the output signal at each time instant  $k = \Delta k + k_0$ ,  $\Delta k \geq 0$ , as

$$y(k) = \left( C \left( \sum_{i=0}^{\Delta k-1} A^i \right) B + D \right) \bar{u} + C A^{\Delta k} X(0) = \left( C \left( \sum_{i=0}^{\Delta k-1} A^i - (I - A)^{-1} \right) B \right) \bar{u} + C A^{\Delta k} X(0),$$

where in the second equality we use the 0 steady state property of the transfer function. Since the matrix  $A$  is stable (i.e.,  $|\lambda(A)| < 1$ ), we have  $(I - A)^{-1} = \sum_{i \geq 0} A^i$ . This equality allows us to simplify the above equality to

$$\begin{aligned}y(k) &= -C \left( \sum_{i=\Delta k}^{\infty} A^i \right) B \bar{u} + C A^{\Delta k} X(0) \\ &= -C A^{\Delta k} \left( \sum_{i=0}^{\infty} A^i \right) B \bar{u} + C A^{\Delta k} X(0) = -C A^{\Delta k} ((I - A)^{-1} B \bar{u}) + C A^{\Delta k} X(0).\end{aligned} \quad (21)$$

We note that the LTI system can be equivalently written as

$$\frac{b(\mathbf{q})}{a(\mathbf{q})} = \frac{\sum_{i=0}^d b_i \mathbf{q}^i}{\prod_{i=1}^d (\mathbf{q} - p_i)} = b_d + \sum_{i=1}^d \frac{r_i}{\mathbf{q} + p_i},$$

where  $r_i$  is as defined in the lemma statement. We further focus on the particular choice of Jordan state-space canonical form in which  $A = \text{diag}\{[p_1, \dots, p_d]\}$ ,  $B = [1, \dots, 1]^\top$ ,  $C = [r_1, \dots, r_n]$ , and

$D = b_d$ . Thanks to diagonal structure of the matrix  $A$ , we have  $\|A\|_2 = |p|$ . Therefore, using the triangle property of norms, the equality (21) yields the bound

$$\begin{aligned}\|y(k)\|_2 &\leq \|C\|_2 \|A\|_2^{\Delta k} (1 - \|A\|_2)^{-1} \|B\|_2 |\bar{u}| + \|C\|_2 \|A\|_2^k \|X(0)\|_2 \\ &= \|C\|_2 |p|^{\Delta k} (1 - |p|)^{-1} \|B\|_2 |\bar{u}| + \|C\|_2 |p|^k \|X(0)\|_2.\end{aligned}$$

The above relation holds for every time instant  $k \in \mathbb{N}$  and  $\Delta k = k - k_0 \geq 0$ . Therefore, we can conclude that

$$\|y_n\| \leq \sqrt{n} \|C\|_2 |p|^{k-k_0-n} (1 - |p|)^{-1} \|B\|_2 |\bar{u}| + \|C\|_2 |p|^{k-n} \|X(0)\|_2,$$

which in case of the special choices of  $B$  and  $C$  implies the desired constants  $\mathcal{C}_0$  and  $\mathcal{C}_1$ . We now focus on the response to the second part  $(u(k) - \bar{u}\delta_{k_0}(k))$  in the input signal (20). Note that the  $\mathcal{L}_2$ -norm of  $u(\cdot) - \bar{u}\delta_{k_0}(\cdot)$  is indeed  $\sqrt{k - k_0} V_{k-k_0}[u]$ . In this view, the constant  $\mathcal{C}_2$  can be upper bounded by the  $\mathcal{H}_\infty$ -norm of the transfer function; recall the  $\mathcal{H}_\infty$ -norm of a transfer function is the  $\mathcal{L}_2$  induced norm of the transfer function as an operator. We then have

$$\mathcal{C}_2 = \left\| \frac{a(\mathbf{q})}{b(\mathbf{q})} \right\|_{\mathcal{H}_\infty} = \sup_{\Omega \in [0, 2\pi]} \left| \frac{a(e^{j\Omega})}{b(e^{j\Omega})} \right| \leq |b_d| + \sum_{i=1}^d \sup_{\Omega \in [0, 2\pi]} \frac{|r_i|}{|e^{j\Omega} - p_i|} \leq |b_d| + \sum_{i=1}^d \frac{|r_i|}{1 - |p_i|},$$

where the second equality follows from a classical result in control theory [2, Theorem 2], the first inequality is due to the triangle inequality, and the second inequality is obtained as the maximum gain is attained from  $\Omega \in \{0, \pi\}$ .  $\square$

#### 4.2. Bounds on variance of product signals

Before proceeding with the proof of the main theorems, we need first provide a useful additional lemma concerning the variance of the product of two signals. The results of this section will later facilitate the proofs of the main theorem in the subsequent section.

**Lemma 4.1** (Variance of product signals). *Consider the discrete-time signals  $a$  and  $b$  over a time-horizon  $n$ . At each time instant, we have*

$$|V_n^2[a + b] - V_n^2[a] - V_n^2[b]| \leq 2 \min \{ \|\mathbf{a}_n\|_2 V_n[b], \|\mathbf{b}_n\|_2 V_n[a] \}, \quad (22a)$$

$$V_n[ab] \leq \sqrt{n} V_n[a] V_n[b] + |\mu_n[a]| V_n[b] + |\mu_n[b]| V_n[a]. \quad (22b)$$

*Proof.* We first note that since the desired assertion holds for everything time instant and horizon  $n$ , the signals  $a, b$  can be viewed as an  $n$ -dimensional vectors. Let us start with the observation that

$$\begin{aligned}V_n^2[a + b] &= \frac{1}{n} \|\mathbf{a}_n + \mathbf{b}_n\|_2^2 - \mu_n^2[a + b] = \frac{1}{n} (\|\mathbf{a}_n\|_2^2 + \|\mathbf{b}_n\|_2^2) + 2\mu_n[ab] - \mu_n^2[a] - \mu_n^2[b] - 2\mu_n[a] \mu_n[b] \\ &= V_n^2[a] + V_n^2[b] + 2\mu_n[ab] - 2\mu_n[a] \mu_n[b] = V_n^2[a] + V_n^2[b] + 2\mu_n[a(b - \mu_n[b])].\end{aligned} \quad (23)$$

Note, that the expression  $\mu_n[a(b - \mu_n[b])]$  is equivalent to the inner product of the last  $n$  time instants of the signals  $a$  and  $(b - \mu_n[b])$  multiplied by the constant  $n$ . By virtue of the Cauchy-Schwarz inequality, for any signals  $v, w$  we have  $|\mu_n[vw]| \leq n \|\mathbf{v}_n\|_2 \|\mathbf{w}_n\|_2$ . This bound together with the equality (23) yields

$$\begin{aligned}V_n^2[a] + V_n^2[b] - 2\|\mathbf{a}_n\|_2 V_n[b] &\leq V_n^2[a + b] \leq V_n^2[a] + V_n^2[b] + 2\|\mathbf{a}_n\|_2 V_n[b], \\ \iff |V_n^2[a + b] - V_n^2[a] - V_n^2[b]| &\leq 2\|\mathbf{a}_n\|_2 V_n[b].\end{aligned}$$



Thanks to the symmetry between  $a$  and  $b$  in the above implication, a possibly less conservative upper-bound can be deduced:

$$|V_n^2[a+b] - V_n^2[a] - V_n^2[b](k)| \leq 2 \min \{ \|\mathbf{a}_n\|_2 V_n[b], \|\mathbf{b}_n\|_2 V_n[a] \}.$$

This concludes the assertion (22a). To show (22b), we define two constants at the given time instant  $k$  as

$$\bar{a} := \mu_n[a](k), \quad \bar{b} := \mu_n[b](k). \quad (24)$$

We emphasize that we view  $\bar{a}, \bar{b}$  as two constants over the entire history, and that we possibly have  $\mu_n[a](k') \neq \bar{a}$  if  $k' < k$ . In other words, the vector  $[\mu_n[a](k-n+1), \dots, \mu_n[a](k)]^\top$  is *not* the same as  $\bar{a} \mathbf{1}_n$ ; these two vectors only agree on the very last component. Using the definitions (24), we have

$$V_n^2[ab] = V_n^2[(a - \bar{a} + \bar{a})(b - \bar{b} + \bar{b})] = V_n^2[(a - \bar{a})(b - \bar{b}) + \bar{b}(a - \bar{a}) + \bar{a}(b - \bar{b}) + \bar{a}\bar{b}]$$

Since the variance operator is invariant under a constant offset, the above relation reduces to

$$V_n^2[ab] = V_n^2[(a - \bar{a})(b - \bar{b}) + \bar{b}(a - \bar{a}) + \bar{a}(b - \bar{b})]. \quad (25)$$

To simplify the notation, let us introduce

$$v := (a - \bar{a})(b - \bar{b}), \quad w := \bar{b}(a - \bar{a}) + \bar{a}(b - \bar{b}). \quad (26)$$

Using the above definitions and the result from (22a), we can derive the following bound from the equality (25):

$$V_n^2[ab] = V_n^2[v+w] \leq V_n^2[v] + V_n^2[w] + 2 \min \{ \|\mathbf{v}_n\|_2 V_n[w], \|\mathbf{w}_n\|_2 V_n[v] \} \quad (27a)$$

$$\leq V_n^2[v] + V_n^2[w] + 2V_n[v]V_n[w] = (V_n[v] + V_n[w])^2, \quad (27b)$$

where the inequality in (27a) is a direction application of (22a), and the inequality in (27b) follows from the fact that the signal  $w$  has a zero mean and thus  $\|\mathbf{w}_n\|_2 = V_n[w]$ . Substituting back the definitions of  $v$  and  $w$  from (26) into the inequality (27b) yields

$$\begin{aligned} V_n^2[ab] &\leq \left( \sqrt{n}V_n[a]V_n[b] + \frac{1}{\sqrt{n}} \|\bar{b}(\mathbf{a}_n - \bar{a}\mathbf{1}_n)\|_2 + \frac{1}{\sqrt{n}} \|\bar{a}(\mathbf{b}_n - \bar{b}\mathbf{1}_n)\|_2 \right)^2 \\ &= \left( \sqrt{n}V_n[a]V_n[b] + \frac{|\bar{b}|}{\sqrt{n}} \|\mathbf{a}_n - \bar{a}\mathbf{1}_n\|_2 + \frac{|\bar{a}|}{\sqrt{n}} \|\mathbf{b}_n - \bar{b}\mathbf{1}_n\|_2 \right)^2 \end{aligned}$$

which concludes the desired assertion (22b) since  $\sqrt{n}V_n[a] = \|\mathbf{a}_n - \bar{a}\mathbf{1}_n\|_2$ .  $\square$

### 4.3. Proofs of the main theorems

*Proof of Theorem 3.5.* Let us first introduce the shorthand notation

$$\mathcal{G} := \mathcal{T} - \mathcal{I}, \quad \delta(k) := f_a + e f_m(k), \quad e = E(z(k)), \quad (28)$$

where the transfer function  $\mathcal{T}$  is as defined in (8) and  $\mathcal{I}$  is the identity transfer function. Notice that in this part the pre-filter is the static gain identity, and that its output signal  $e$  is indeed the measurement signal  $E(z)$  (cf. Figure 1). Based on the definition of the estimated fault and the regression operator in Definition 3.2 we have

$$\hat{f} = \Phi_n[e, r] = \Phi_n[e, r - \delta] + \Phi_n[e, \delta] - \mu_n[f] + \mu_n[f],$$

where the second equality simply follows from the linearity of the regression operator in the second argument. Let moving the term  $\mu_n[f]$  to the left-hand side and taking the 2-norm on both sides of the above equality. Using the triangle inequality and the regression bounds from Proposition 3.3, we arrive at

$$\begin{aligned} \|\hat{f} - \mu_n[f]\|_2 &\leq \|\Phi_n[e, r - \delta]\|_2 + \|\Phi_n[e, \delta] - \mu_n[f]\|_2 \\ &\leq \frac{\mathcal{C}_n(\mathbf{e}_n)}{\sqrt{n}V_n[e]}\|\mathbf{r}_n - \delta_n\|_2 + \frac{\mathcal{C}_n(\mathbf{e}_n)}{V_n[e]}(V_n[f_a] + V_n[f_m]\|\mathbf{e}_n\|_\infty), \end{aligned} \quad (29)$$

where the first and second bounds in (29) follow from (11b) and (11a), respectively. It then remains to bound the term  $\|\mathbf{r}_n - \delta_n\|_2$  on the right-hand side of (29). Following the definitions of the residual  $r$  in (8), and the signal  $\delta$  and the transfer function  $\mathcal{G}$  in (28), we have

$$r - \delta = \mathcal{T}[f_a + E(z)f_m] - (f_a + ef_m) = \mathcal{G}[f_a] + \mathcal{G}[ef_m].$$

Note that by construction the transfer function  $\mathcal{G}$  has a zero steady-state gain since the transfer function  $\mathcal{T}$  has *unit* steady-state gain (see Lemma 3.1). As such, we can apply Lemma 3.4 to the right-hand side of the above relation. This leads to

$$\begin{aligned} \|\mathbf{r}_n - \delta_n\|_2 &\leq \mathcal{C}_1(|\mu_{k-k_0}[f_a]| + |\mu_{k-k_0}[ef_m]|)|p|^{k-k_0} + \mathcal{C}_2\sqrt{k-k_0}(V_{k-k_0}[f_a] + V_{k-k_0}[ef_m]), \\ &\leq \mathcal{C}_1(|\mu_{k-k_0}[f_a]| + |\mu_{k-k_0}[ef_m]|)|p|^{k-k_0} + \mathcal{C}_2\sqrt{k-k_0}\left(V_{k-k_0}[f_a] \right. \\ &\quad \left. + \sqrt{k-k_0}V_{k-k_0}[f_m]V_{k-k_0}[e] + |\mu_{k-k_0}[f_m]|V_{k-k_0}[e] + |\mu_{k-k_0}[e]|V_{k-k_0}[f_m]\right), \end{aligned}$$

where in the last line we apply (22b) from Lemma 4.1 to the variance of the product signals  $V_{k-k_0}[ef_m]$ . Substituting the above bound in (29) results in

$$\begin{aligned} \|\hat{f} - \mu_n[f]\|_2 &\leq \frac{\mathcal{C}_n(\mathbf{e}_n)}{\sqrt{n}V_n[e]}\left(\mathcal{C}_1(|\mu_{k-k_0}[f_a]| + |\mu_{k-k_0}[ef_m]|)|p|^{k-k_0} \right. \\ &\quad \left. + \mathcal{C}_2\sqrt{k-k_0}(V_{k-k_0}[f_a] + \sqrt{k-k_0}V_{k-k_0}[f_m]V_{k-k_0}[e] \right. \\ &\quad \left. + |\mu_{k-k_0}[f_m]|V_{k-k_0}[e] + |\mu_{k-k_0}[e]|V_{k-k_0}[f_m])\right) + \frac{\mathcal{C}_n(\mathbf{e}_n)}{V_n[e]}(V_n[f_a] + V_n[f_m]\|\mathbf{e}_n\|_\infty). \end{aligned}$$

Finally, it suffices to factor out the right-hand side of the above inequality to the exponentially decaying term and the variance terms  $V_{k-k_0}[f_a]$ ,  $V_{k-k_0}[f_m]$ , as well as the remaining parts including  $V_n[f_a]$ ,  $V_n[f_m]$ ,  $V_{k-k_0}[e]$ . This concludes the desired assertion (12).  $\square$

*Proof of Theorem 3.5.* The key difference between the setting of this theorem with Theorem 3.5 is the choice of pre-filter, and as such, the definition of the signal  $e$ . Consider the same definitions of the transfer function  $\mathcal{G}$  and the signal  $\delta$  as in (28) where the output of the pre-filter is defined as

$$e = \mathcal{T}[E(z)], \quad \text{with the internal states } X_p. \quad (30)$$

Note that the relation (29) still holds in the setting here as well. We then only need focus on the term  $\|\mathbf{r}_n - \delta_n\|_2$ . In the rest of the proof, we fix the time instant  $k \in \mathbb{N}$  and define the average of the multiplicative fault  $f_m$  over the horizon  $[k-n, k]$  as the constant denoted by

$$\overline{f_m} := \mu_n[f_m](k). \quad (31)$$

Let us emphasize that we view the value  $\overline{f_m}$  as constant over the entire time horizon prior to  $k$ ; see also the definitions (24) and the following paragraph there. We further introduce the shorthand notation of the step function

$$\mathfrak{U}_{k_0}(k) := \begin{cases} 0 & k < k_0 \\ 1 & k \geq k_0. \end{cases}$$

Following the above definitions, the signal  $r - \delta$  can be rewritten as

$$\begin{aligned} r - \delta &= \mathcal{T}[f_a + E(z)f_m] - (f_a + \mathcal{T}[E(z)]f_m) = \mathcal{G}[f_a] + \mathcal{T}[E(z)f_m] - \mathcal{T}[E(z)]f_m \\ &= \mathcal{G}[f_a] + \mathcal{T}[E(z)f_m - \overline{f_m}E(z)\mathfrak{U}_{k_0}] + \mathcal{T}[\overline{f_m}E(z)\mathfrak{U}_{k_0}] - \mathcal{T}[E(z)]f_m \\ &= \mathcal{G}[f_a] + \mathcal{T}[E(z)(f_m - \overline{f_m}\mathfrak{U}_{k_0})] + \overline{f_m}\mathcal{T}[E(z)(\mathfrak{U}_{k_0} - 1)]\mathfrak{U}_{k_0} - \mathcal{T}[E(z)](f_m - \overline{f_m}\mathfrak{U}_{k_0}) \quad (32a) \end{aligned}$$

$$= \mathcal{G}[f_a] + \mathcal{G}[E(z)(f_m - \overline{f_m}\mathfrak{U}_{k_0})] + \overline{f_m}\mathcal{T}[E(z)(\mathfrak{U}_{k_0} - 1)]\mathfrak{U}_{k_0} - \mathcal{G}[E(z)](f_m - \overline{f_m}\mathfrak{U}_{k_0}), \quad (32b)$$

where in (32a) we take the constant  $\overline{f_m}$  outside the linear transfer function  $\mathcal{T}$ . We also note that to arrive at (32a) we use the fact that  $\mathcal{T}[E(z)\mathfrak{U}_{k_0}](k) = 0$  for all time instants  $k < k_0$ , i.e.,  $\mathcal{T}[E(z)\mathfrak{U}_{k_0}] = \mathcal{T}[E(z)\mathfrak{U}_{k_0}]\mathfrak{U}_{k_0}$ . Recall that  $\mathcal{G} = \mathcal{T} - \mathcal{I}$  is a stable transfer function with zero steady-state gain. Also, note that for  $k \geq k_0$  the third term  $\mathcal{T}[E(z)(\mathfrak{U}_{k_0} - 1)]$  in (32b) is in fact the contribution of the internal states  $X_p(k_0)$  of the transfer function  $\mathcal{T}$  when the input signal is  $E(z)$  ( $\mathfrak{U}_{k_0} - 1 = 0$  for all  $k \geq 0$ ). Therefore, we can apply Lemma 3.4 to each term on the right-hand side in (32b) and obtain the bound

$$\begin{aligned} \|\mathbf{r}_n - \delta_n\|_2 &\leq \mathcal{C}_1|\overline{f_a}||p|^{k-k_0} + \mathcal{C}_2\sqrt{k-k_0}V_{k-k_0}[f_a] \\ &\quad + \mathcal{C}_1|\mu_{k-k_0}[E(z)(f_m - \overline{f_m}\mathfrak{U}_{k_0})]||p|^{k-k_0} + \mathcal{C}_2\sqrt{k-k_0}V_{k-k_0}[E(z)(f_m - \overline{f_m}\mathfrak{U}_{k_0})] \\ &\quad + |\overline{f_m}|\mathcal{C}_0\|X_p(k_0)\|_2|p|^{k-k_0} \\ &\quad + \|\mathbf{e}_n - E(\mathbf{z}_n)\|_\infty\sqrt{n}V_n[f_m] \end{aligned} \quad (33)$$

We first note that in (33) we can simplify the first term of the second line as  $\mu_{k-k_0}[E(z)(f_m - \overline{f_m}\mathfrak{U}_{k_0})] = \mu_{k-k_0}[E(z)f_m] - \mu_{k-k_0}[E(z)]\overline{f_m}$ . We further borrow the results of Lemma 4.1 to bound the terms involving the product of two signals in (33). More specifically, we have

$$\begin{aligned} V_{k-k_0}[E(z)(f_m - \overline{f_m}\mathfrak{U}_{k_0})] &\leq \sqrt{k-k_0}V_{k-k_0}[E(z)]V_{k-k_0}[f_m] \\ &\quad + |\mu_{k-k_0}[f_m - \overline{f_m}\mathfrak{U}_{k_0}]|V_{k-k_0}[E(z)] + |\mu_{k-k_0}[E(z)]|V_{k-k_0}[f_m] \\ &= \sqrt{k-k_0}V_{k-k_0}[E(z)]V_{k-k_0}[f_m] \\ &\quad + |\mu_{k-k_0}[f_m] - \overline{f_m}\mathfrak{U}_{k_0}|V_{k-k_0}[E(z)] + |\mu_{k-k_0}[E(z)]|V_{k-k_0}[f_m]. \end{aligned} \quad (34)$$

It now suffices to substitute the upper bounds (34) in (33), and then invoke the resulting bound on  $\|\mathbf{r}_n - \delta_n\|_2$  in (29). Finally, it remains to factor out the right-hand side of the inequality to the exponentially decaying term, the variance terms  $V_{k-k_0}[f_a]$ ,  $V_{k-k_0}[f_m]$ , as well as the remaining parts including  $V_n[f_a]$ ,  $V_n[f_m]$ ,  $V_{k-k_0}[E(z)]$ . This concludes the desired assertion (14).  $\square$

## 5. CASE STUDY: LATERAL CONTROL OF AUTONOMOUS VEHICLES

In this section, the presented theory is illustrated using a fault isolation problem in the scope of the lateral control of autonomous vehicles. In this scope, the linear single-track vehicle model is used as a benchmark example [18, Equation 1]. The model represents a linearization of the lateral dynamics of an automated vehicle. As more driver tasks are alleviated in the context of automated driving, the responsibility of passenger safety is expected to shift towards the automated driving software. In this context, fault detection and isolation are increasingly important in the automotive industry [4]. Namely, robustness for failures from both known and unknown sources remains a challenging topic in this domain and requires extensive research and rigorous experimental evaluation [13]. The outline of this section is as follows: first, a model description is given in Section 5.1, simulation results will be shown and a conclusion will be drawn regarding filter performance and bound analysis in Section 5.2. Finally, a sensitivity analysis is performed to explore the degrees of freedom in the filter design in Section 5.3.

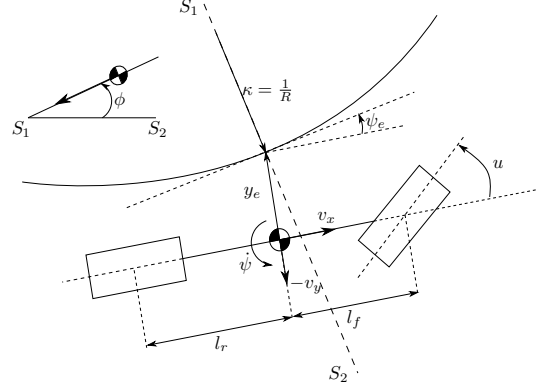


FIGURE 2. Visual representation of the bicycle model.

### 5.1. Problem description

The proposed linear bicycle model is depicted in Figure 2. Here, the state of the vehicle is chosen as  $X = [v_y, \dot{\psi}, y_e, \psi_e]^T$  where  $v_y$  represents the lateral velocity,  $\dot{\psi}$  represents the yaw-rate,  $y_e$  represents the lateral error from the lane centre and  $\psi_e$  represents the heading error from the lane centre. The disturbance vector is chosen as  $d = [\sin(\phi), \kappa]$  where  $\phi$  represents the banking angle of the road (as depicted by cross-section  $S_1 - S_2$  in Figure 2) and  $\kappa$  represents the curvature of the road. The input  $u$  represents the steering wheel angle of the front wheels of the vehicle. In this case-study, we consider additive and multiplicative faults acting on the steering input signal  $u$ . These faults could realistically occur as an offset in the steering column,  $f_a$ , or a loss of actuator efficiency,  $f_m$ . These faults may result in unexpected transient and steady-state tracking errors and hence result in dangerous situations for the vehicle passengers if not detected and handled properly. The model description with its states, disturbances, faults and input can be written in the form of a continuous-time, linear differential equation as follows:

$$\begin{cases} \dot{X}(t) = \bar{A}X(t) + \bar{B}_u u(t) + \bar{B}_f(f_m(t)u(t) + f_a(t)) + \bar{B}_d d(t), \\ Y(t) = CX, \end{cases} \quad (35)$$

where the system matrices  $\bar{A}$ ,  $\bar{B}_u$ ,  $\bar{B}_d$ ,  $C$  can be written as follows [18, Equation 1]:

$$\bar{A} = \begin{bmatrix} \frac{C_f + C_r}{v_x m} & \frac{l_f C_f - l_r C_r}{v_x m} & 0 & 0 \\ \frac{l_f C_f - l_r C_r}{v_x I} & \frac{l_f^2 C_f + l_r^2 C_r}{v_x I} & 0 & 0 \\ -1 & 0 & 0 & v_x \\ 0 & -1 & 0 & 0 \end{bmatrix}, \quad \bar{B}_u = \begin{bmatrix} -\frac{C_f}{I} \\ -\frac{l_f C_f}{I} \\ 0 \\ 0 \end{bmatrix}, \quad \bar{B}_d = \begin{bmatrix} g & 0 \\ 0 & 0 \\ 0 & 0 \\ 0 & v_x \end{bmatrix}, \quad C = \begin{bmatrix} 0 & 1 & 0 & 0 \\ 0 & 0 & 1 & 0 \\ 0 & 0 & 0 & 1 \end{bmatrix},$$

where  $C_f = 1.50 \cdot 10^5 \text{ N} \cdot \text{rad}^{-1}$  and  $C_r = 1.10 \cdot 10^5 \text{ N} \cdot \text{rad}^{-1}$  represent the lateral cornering stiffnesses of the front and rear tyres, respectively,  $l_f = 1.3 \text{ m}$  and  $l_r = 1.7 \text{ m}$  represent the distances from the front and rear axle to the center of gravity, respectively,  $v_x = 19 \text{ m} \cdot \text{s}^{-1}$  represents the longitudinal velocity,  $m = 1500 \text{ kg}$  represents the total mass of the vehicle,  $I = 2600 \text{ kg} \cdot \text{m}^2$  represents the moment of inertia around the vertical axis of the vehicle and finally  $g = 9.81 \text{ m} \cdot \text{s}^{-2}$  represents the gravitational acceleration. In order to fit the discrete-time model setting employed in this paper, we first exactly discretize the dynamical system using a classical control theoretical result [25, Section 2]. The resulting discrete-time state-space matrices can be written as follows:

$$\begin{cases} A = e^{\bar{A}h}, & B_u = \int_0^h e^{\bar{A}s} \bar{B}_u ds, \\ B_d = \int_0^h e^{\bar{A}s} \bar{B}_d ds, & B_f = \int_0^h e^{\bar{A}s} \bar{B}_f ds, \end{cases} \quad (36)$$

where  $h$  is the sampling interval and is chosen as  $h = 0.01 \text{ s}$  and  $f = f_m u + f_a$  represents the aggregated fault signal. Note, that the discretized system matrices (36) can be written in the DAE framework by virtue of Fact 2.1 when setting  $K_X = 0$  and  $K_Y = 0$ .

## 5.2. Simulation results

For the synthesis of the fault detection filter, the degree of the filter  $N(\mathbf{q})$  is set to  $d_N = 3$ . The denominator  $a(\mathbf{q})$  of the fault detection filter is set to  $a(\mathbf{q}) = (\mathbf{q} + 0.85)(\mathbf{q} + 0.59)(\mathbf{q} + 0.58)$ . Note, that distinct poles are chosen to be able to verify the performance bound of the estimation error using the results of Lemma 3.4. The filter  $N(\mathbf{q})$  can be found by solving the linear program in (9). For synthesis of the fault isolation filter, the time horizon  $n$  is initially chosen as  $n = 10$ . This forms a basis for the fault diagnosis filter.

The input signal  $u$  to the system dynamics is selected to be a sinusoidal signal with an amplitude of  $2.3 \cdot 10^{-3}$  radians at a frequency of 0.3Hz. The frequency content of the input signal is inspired by experimental data of an automated vehicle, driving in-lane using a PD-type controller, while being excited by natural disturbances (e.g., profile of the road). The faults  $f_a, f_m$  are selected as piecewise linear functions:

$$f_a(k) := \begin{cases} 0 & 0 \leq k < 100 \\ 0.1 \frac{\pi}{180} & 100 \leq k \leq 500 \end{cases}, \quad f_m(k) := \begin{cases} 0 & 0 \leq k < 300 \\ -0.2 & 300 \leq k \leq 500 \end{cases}.$$

These fault functions are chosen to realistically correspond to an experimental setting. The additive fault  $f_a$  usually appears as a low magnitude fault as it could be caused by a small mechanical misalignment in the steering rack. The multiplicative fault  $f_m$  is chosen to represent a degradation of the efficiency of the steering actuator. This is a critical case in automated driving as a continuously degrading actuator could result in a decision to park towards the side of the road. The practical value of the faults and the system described shows the particular value of this simulation setup. Using the described model and its inputs, the two faults are injected and the estimation error and performance bounds from Theorem 3.5 and 3.7 are simulated/evaluated as shown in Figure 3.

Figure 3a and 3b show the injected faults  $f_a$  and  $f_m$  as well as the estimated faults  $\hat{f}_a$  and  $\hat{f}_m$  using a static and dynamic pre-filter, respectively. As shown in Figure 3a and 3b, the fault estimates  $\hat{f}_a, \hat{f}_m$  from the diagnosis filter with static pre-filter (Theorem 3.7) fluctuate heavily around the true

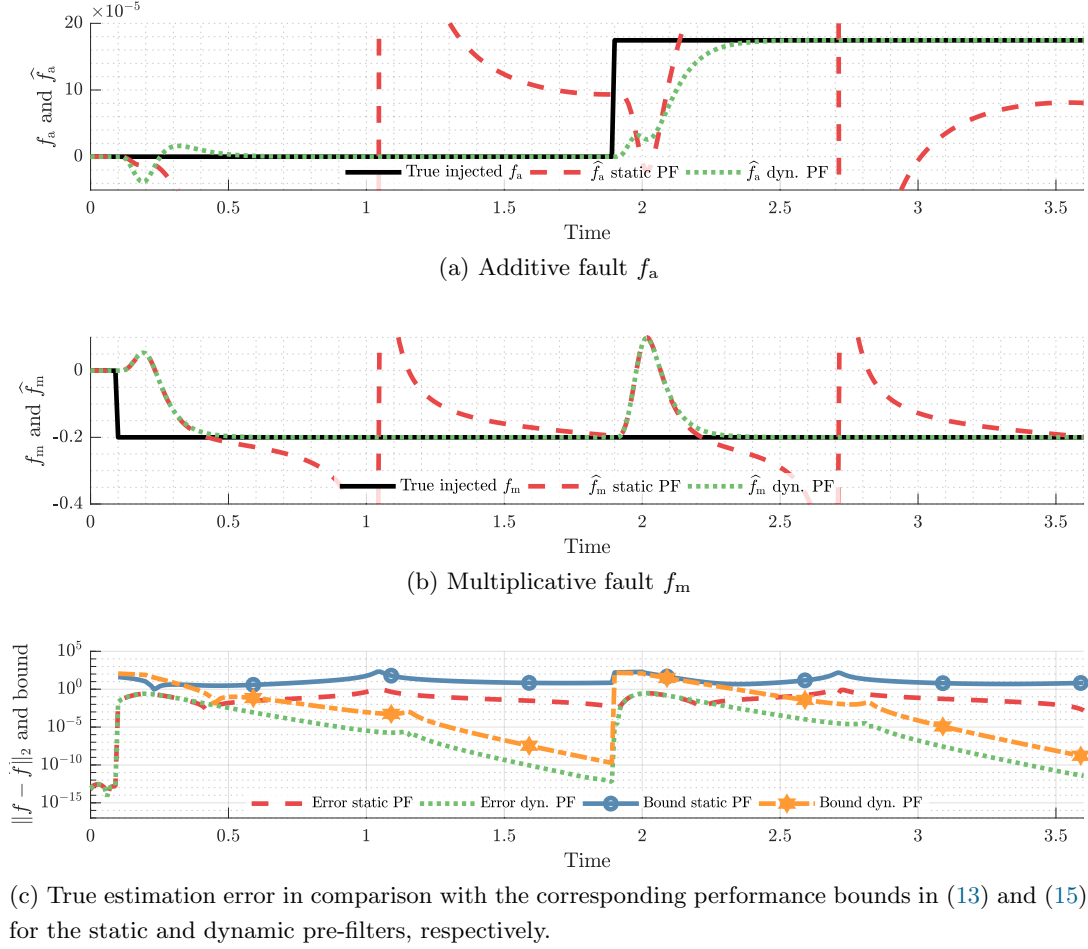


FIGURE 3. True estimation errors and the corresponding performance bounds in the presence of constant faults as discussed in Corollaries 3.6 and 3.8 (PF: Pre-Filter).

injected fault. This particular behavior is also reflected by the performance bound in the constant-fault case as depicted in Corollary 3.6, where we find that in particular the variance of the signal  $e$  (in this case-study, we consider  $E(z) = u$ , hence  $e$  is either a direct feed through or filtered version of  $u$ ) is a persistent contributor in the bound of the estimation error. As a matter of fact, the periodic behavior of the estimated faults is found to be oscillating with the same period as input signal  $u$ . The estimated faults that result from the diagnosis filter with the dynamic pre-filter (Theorem 3.7) show convergence to the constant true faults over time. This was to be expected, as it was shown in Corollary 3.8 that, in the constant fault-case, the performance bound decays exponentially as time increases. Figure 3c depicts the estimation errors (left-hand side of (12a) and (14a) for the static pre-filter and the dynamic pre-filter, respectively) and their simulated performance bounds (right-hand side of (12a) and (14a) for the static pre-filter and the dynamic pre-filter, respectively). It can be observed from this figure that the estimation error and its performance bound for the static pre-filter are time-varying and non-zero, even for constant faults. This confirms our findings from Corollary 3.6, where it was shown that the performance bound for constant faults always

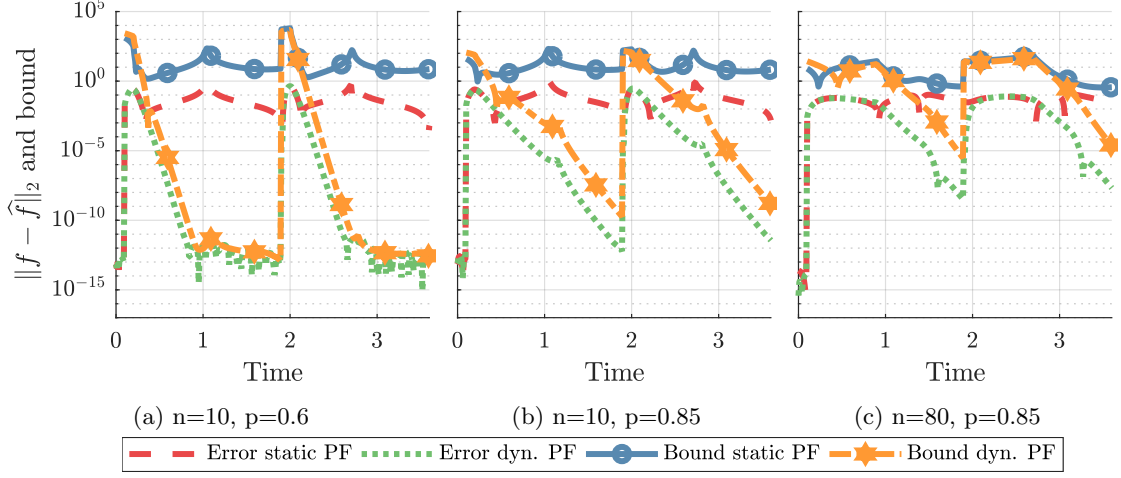


FIGURE 4. Sensitivity of true estimation errors and the corresponding performance bounds proposed by Corollaries 3.6 and 3.8 with respect to the dominant pole  $p$  and the regression horizon  $n$  (PF:Pre-Filter).

depends on  $V_{k-k_0}[e]$  which was assumed to be non-zero. The estimation error shows similar non-zero behavior, showing that the bound gives sufficient insight in the behavior of the estimation error. For the dynamic pre-filter, the performance bound and the estimation error drop towards zero (up to numerical precision) when the fault is constant and the pre-filter has converged. Once a new fault occurs, the estimation error and its performance bound increase and subsequently converge back towards zero. Translating these results back into the application-perspective of automated driving shows that, both the additive and multiplicative fault, can be estimated simultaneously in a matter of seconds (depending on the tuning of the horizon  $n$  and the poles of the FD filter). This allows the automated vehicle to act upon two different fault-types accordingly, as opposed to having to conservatively act on the presence of an aggregated fault signal  $f_a + e f_m$  without knowing the separate contributions of the faults. For example, a slight offset  $f_a$  in the system could be attenuated in closed loop, a large degradation  $f_m$  however should result in a transition of the vehicle to a safe state.

### 5.3. Sensitivity study

A sensitivity design is done in this section to touch upon potential degrees of freedom that could affect the estimation error of the fault diagnosis filter. The composed bounds in (12) and (14) consist of elements that usually can not be affected in an open-loop system (i.e., the behavior of the faults  $f_a$ ,  $f_m$  and the signal  $e$ ) and those that can be influenced (i.e., the fault detection filter dynamics and the fault isolation time-horizon  $n$ ). In this sensitivity study, the dynamics of the detection filter as well as the horizon  $n$  of the isolation filter are considered as "tuning" parameters. For the fault detection filter dynamics, only the dominant pole  $p$  is considered as a tuning parameter for the sake of simplicity. Figure 4 provides the results of the sensitivity analysis. In Figure 4b, the baseline simulation that was shown in Figure 3c is provided for means of comparison. In Figure 4a, the dominant pole location is shifted from  $p = 0.85$  to  $p = 0.6$ . From the composed performance



bounds (12) and (14) it is clear that, for the performance bound, this strengthens the exponential decay of the average behavior of the faults which can in particular be observed in the convergence behavior of the dynamic pre-filter estimation and bound. When increasing the time-horizon  $n$  from  $n = 10$  to  $n = 80$  it is clearly observed in Figure 4c that the bound is pushed down and, as a result, the estimation error is also pushed down. This was to be expected, as the horizon  $n$  forms a common denominator for a large part of both performance bounds. However, the exponential decay of the average behavior is slower due to its influence on the average behavior in (12) and (14). There are more, less trivial, phenomena caused by a change in parameters  $n$  and  $p$ . The effects of these phenomena will not be investigated in this analysis as the effects are highly dependent on the signal properties of signals  $f_a$ ,  $f_m$  and  $e$  and it is therefore difficult to assess generically.

## 6. CONCLUSION AND FUTURE DIRECTIONS

In this work, a fault diagnosis architecture for the detection, isolation and estimation of additive and multiplicative faults is presented. System-theoretic bounds have been developed for the regression operator. These bounds, including several preliminary lemmas have proven to be valuable building blocks for the composition of guaranteed performance bounds for the detection, isolation and estimation architecture for two particular variants of the pre-filter block. The insights gained from the first pre-filter variant (i.e., the identity block) and its behavior for constant faults have been used for design of a second variant (i.e., the dynamic pre-filter) which has been proven to have an asymptotically decaying bound for constant faults. Simulation results in the domain of SAE level 4 automated driving shows the practical value and the potential of the proposed approach in relevant future-proof applications.

A future research direction is the closed-loop implementation of the proposed diagnosis filter. We envision that this could be a stepping-stone towards a class of fault tolerant control systems that enjoys rigorous stability and performance guarantees. Another interesting direction is the application the proposed diagnosis architecture in an active fault diagnosis context. This could also build on the key insights obtained from the performance bounds with a particular focus on the role of signals characteristics. Moreover, it is also worth noting that a probabilistic treatment towards the effects of measurements noise (e.g., the  $\mathcal{H}_2$  gain of the noise to residual as in [20]) could also be another direction.

## REFERENCES

- [1] A. Ansari and D.S. Bernstein. Deadbeat unknown-input state estimation and input reconstruction for linear discrete-time systems. *Automatica*, 103:11–19, 2019.
- [2] B. Bamieh and J. Boyd Pearson. A general framework for linear periodic systems with applications to  $\mathcal{H}_\infty$  sampled-data control. *IEEE Transactions on Automatic Control*, 37(4):418–435, 1992.
- [3] R.V. Beard. *Failure Accommodation in Linear Systems Through Self-reorganization*. NASA CR. M.I.T. Man-Vehicle Laboratory, 1971.
- [4] K. Bengler, K. Dietmayer, B. Farber, M. Maurer, C. Stiller, and H. Winner. Three decades of driver assistance systems: Review and future perspectives. *IEEE Intelligent Transportation Systems Magazine*, 6(4):6–22, 2014.
- [5] F. Boem, R.M.G. Ferrari, and T. Parisini. Distributed fault detection and isolation of continuous-time non-linear systems. *European Journal of Control*, 17(5-6):603–620, 2011.

- [6] F. Boem, S. Rivero, G. Ferrari-Trecate, and T. Parisini. Plug-and-play fault detection and isolation for large-scale nonlinear systems with stochastic uncertainties. *IEEE Transactions on Automatic Control*, 64(1):4–19, 2019.
- [7] L. Chen, S. Fu, Y. Zhao, M. Liu, and J. Qiu. State and fault observer design for switched systems via an adaptive fuzzy approach. *IEEE Transactions on Fuzzy Systems*, 28(9):2107–2118, 2020.
- [8] M. Du and P. Mhaskar. Isolation and handling of sensor faults in nonlinear systems. *Automatica*, 50(4):1066 – 1074, 2014.
- [9] P.M. Esfahani and J. Lygeros. A tractable fault detection and isolation approach for nonlinear systems with probabilistic performance. *IEEE Transactions on Automatic Control*, 61(3):633–647, 2016.
- [10] Z. Gao, C. Cecati, and S. X. Ding. A survey of fault diagnosis and fault-tolerant techniques—part ii: Fault diagnosis with knowledge-based and hybrid/active approaches. *IEEE Transactions on Industrial Electronics*, 62(6):3768–3774, 2015.
- [11] Z. Gao, C. Cecati, and S.X. Ding. A survey of fault diagnosis and fault-tolerant techniques-part i: Fault diagnosis with model-based and signal-based approaches. *IEEE Transactions on Industrial Electronics*, 62(6):3757–3767, 2015.
- [12] J. Gertler. Fault detection and isolation using parity relations. *Control Engineering Practice*, 5(5):653 – 661, 1997.
- [13] J. Guanetti, Y. Kim, and F. Borrelli. Control of connected and automated vehicles: State of the art and future challenges. *Annual Reviews in Control*, 45:18 – 40, 2018.
- [14] R. Iqbal, T. Maniak, F. Doctor, and C. Karyotis. Fault detection and isolation in industrial processes using deep learning approaches. *IEEE Transactions on Industrial Informatics*, 15(5):3077–3084, 2019.
- [15] F. Jia, Y. Lei, J. Lin, X. Zhou, and N. Lu. Deep neural networks: A promising tool for fault characteristic mining and intelligent diagnosis of rotating machinery with massive data. *Mechanical Systems and Signal Processing*, 72-73:303 – 315, 2016.
- [16] M. Nyberg and E. Frisk. Residual generation for fault diagnosis of systems described by linear differential-algebraic equations. *IEEE Transactions on Automatic Control*, 51(12):1995–2000, 2006.
- [17] K. Pan, P. Palensky, and P. M. Esfahani. From static to dynamic anomaly detection with application to power system cyber security. *IEEE Transactions on Power Systems*, 35(2):1584–1596, 2020.
- [18] A. Schmeitz, J. Zegers, J. Ploeg, and M. Alirezaei. Towards a generic lateral control concept for cooperative automated driving theoretical and experimental evaluation. In *2017 5th IEEE International Conference on Models and Technologies for Intelligent Transportation Systems (MT-ITS)*, pages 134–139. IEEE, 2017.
- [19] I. Shames, A.M.H. Teixeira, H. Sandberg, and K.H. Johansson. Distributed fault detection for interconnected second-order systems. *Automatica*, 47(12):2757–2764, 2011. cited By 251.
- [20] B. Svetozarevic, P.M. Esfahani, M. Kamgarpour, and J. Lygeros. A robust fault detection and isolation filter for a horizontal axis variable speed wind turbine. *Proceedings of the American Control Conference*, pages 4453–4458, 2013.
- [21] C.P. Tan and C. Edwards. Multiplicative fault reconstruction using sliding mode observers. *2004 5th Asian Control Conference*, 2:957–962, 2004. cited By 26.
- [22] T. Van Gestel, J.A.K. Suykens, B. Baesens, S. Viaene, J. Vanthienen, G. Dedene, B. De Moor, and J. Vandewalle. Benchmarking least squares support vector machine classifiers. *Machine Learning*, 54(1):5–32, 2004.
- [23] H. Wang and S. Daley. Actuator fault diagnosis: An adaptive observer-based technique. *IEEE Transactions on Automatic Control*, 41(7):1073–1078, 1996.
- [24] Jan C. Willems, Paolo Rapisarda, Ivan Markovsky, and Bart L.M. De Moor. A note on persistency of excitation. *Systems & Control Letters*, 54(4):325 – 329, 2005.
- [25] Y. Yamamoto and P.P. Khargonekar. Frequency response of sampled-data systems. *IEEE Transactions on Automatic Control*, 41(2):166–176, 1996.
- [26] M. Yu, C. Xiao, W. Jiang, S. Yang, and H. Wang. Fault diagnosis for electromechanical system via extended analytical redundancy relations. *IEEE Transactions on Industrial Informatics*, 14(12):5233–5244, 2018.
- [27] T. Zhan, J. Tian, and S. Ma. Full-order and reduced-order observer design for one-sided lipschitz nonlinear fractional order systems with unknown input. *International Journal of Control, Automation and Systems*, 16(5):2146–2156, 2018.